

## Effects of $\rho$ exchange in coherent pion production

P. A. Deutchman and F. Sammarruca

*Department of Physics, University of Idaho, Moscow, Idaho 83844-0903*

(Received 21 October 1996; revised manuscript received 28 July 1997)

New theoretical calculations have been done that compare  $\pi$ - and  $\rho$ -exchange effects in exclusive coherent production of pions for  $^{12}\text{C}+^{12}\text{C}\rightarrow^{12}\text{C}+^{12}\text{C}+\pi^0$  below and above the pion threshold at incident energies of 100, 250, and 400 MeV/nucleon. Besides the important enhancement effects to the pion distributions due to the constructive coherence of  $\Delta$ -hole and particle-hole terms describing the coherent, intermediate nuclear states of both projectile and target, additional effects have been observed due to the  $\rho$ -exchange transition interaction. Calculations of the pion angular distributions, which are sensitive to the  $\rho$ -exchange effect, are done that compare the  $(\pi+\rho)$ -exchange effects to the  $\pi$ -exchange effect alone. It is shown that at extreme angles, where the projectile scatters forward ( $\Theta_p=0^\circ$ ), and the target scatters backward ( $\Theta_T=180^\circ$ ), and the pion scattering forward or backward ( $\theta_\pi=0^\circ$  or  $180^\circ$ ), that the  $\rho$  amplitude is zero under the Born approximation. The insensitivity of the pion-energy distributions to  $\rho$  exchange is also explained. It is shown that the  $\rho$ -exchange effect is a rather mild one which affects only the midregion of the pion-angular distributions for the particular physical channels and incident energies considered here. [S0556-2813(98)01901-3]

PACS number(s): 25.70.-z, 24.10.Cn, 24.30.Cz

### I. INTRODUCTION

There is continued interest in coherent pion production theoretically, especially as to how this production relates to the  $\Delta$ -hole mechanism as well as to the longitudinal and transverse properties of the  $\Delta$ -generating interactions [1–5]. These investigations have been concerned with charge-exchange reactions with nuclear probes such as  $(p,n)$  or  $(^3\text{He},t)$  at intermediate energies. Our work has concentrated on constructive coherent pion production with equal mass, “welterweight” ions such as  $^{12}\text{C}+^{12}\text{C}$  at energies above and below the pion threshold. However, a complete isospin formalism has been included which makes it possible to study charge-exchange and nonexchange reactions, and furthermore, unequal mass nuclei can be considered.

This paper is a continuation of a series of papers [6–11] that describes quantum-mechanical constructive coherence in the production of pions from the collision of two equal mass nuclei at energies around the pion threshold. It is of great interest to ascertain which physical effects in the theoretical description provide various signatures of coherent pion production over a range of incident energies above and below the pion threshold. This then tells us how to “read” the pion energy, and angular distributions and relates the physical effects to various parts of the pion distributions. Briefly, the present theoretical description involves the solution in a three-coordinate, partial-wave expansion of the second-order amplitudes in the Born approximation of the projectile- and target-generated pions. One amplitude describes the virtual excitation of  $\Delta$ -hole states in one nucleus, while ordinary particle-hole states are excited in the other, and a second amplitude describes the exchange process. Both nuclei are excited into spin-isospin giant resonances. The excitation of the virtual  $\Delta$  particle is mitigated by  $\pi$ - and  $\rho$ -exchange transition interactions and the  $\Delta$  particle then resonates through an energy-dependent width. Finally, a decay amplitude describes the decay of the  $\Delta$  to a nucleon and pion. These details have been described in previous papers [6,8,9].

The first major effect to the shapes of the pion distributions is due to the *constructive interference* in the sum of  $\Delta$ -hole and particle-hole terms that describe the excited-state nuclear form factors. These form factors and their enhancements on the pion-energy distributions have been assessed in a previous paper [9] and it was seen that constructive coherence greatly increases the magnitudes and affects the shapes of the pion-energy distributions over a range of incident energies. Since coherence enhancement of the excited nuclear states has been discussed, we will not dwell upon this effect any further. New calculations have been done to determine the importance of  $\rho$ -exchange effects as compared to  $\pi$ -exchange effects to the pion distributions and is discussed in Sec. II. The conclusions as to the mild enhancement in the pion angular distributions due to the  $\rho$ -exchange effect for the particular physical channels chosen in the calculation are discussed in Sec. III.

### II. $\rho$ -EXCHANGE EFFECTS

The transition interactions for  $nn\rightarrow n\Delta$  used in this work were obtained from Machleidt [12]. To first order, the terms involving the coupling constant  $g_\rho$  of the  $\rho$ -exchange transition interaction (see Eq. (B.4) in Ref. [12]) were neglected since these terms are almost an order of magnitude less than terms involving the coupling constant  $f_\rho$ . The  $\pi$ -exchange and  $\rho$ -exchange interactions in momentum space as a function of momentum transfer  $\mathbf{K}$  are coherently added to give the overall transition interaction between nucleons as

$$v(\mathbf{K})=[v_\pi(\mathbf{K})+v_\rho(\mathbf{K})](\boldsymbol{\tau}_p\cdot\mathbf{T}_\Delta), \quad (1)$$

where the  $\pi$ - and  $\rho$ -exchange interactions are

$$v_\pi(\mathbf{K})=v_\pi(K)(\boldsymbol{\sigma}_p\cdot\hat{\mathbf{K}})(\mathbf{S}_\Delta\cdot\hat{\mathbf{K}}) \quad (2a)$$

and

$$v_\rho(\mathbf{K})=v_\rho(K)(\boldsymbol{\sigma}_p\times\hat{\mathbf{K}})\cdot(\mathbf{S}_\Delta\times\hat{\mathbf{K}}). \quad (2b)$$

TABLE I. Parameters of the transition interactions.

$\alpha$	$m_\alpha$ (MeV)	$f_\alpha^2/4\pi\hbar c$ (unitless)	$\Lambda_\alpha$ (GeV)	$n_\alpha$
$n$	938.926			
$\pi$	138.034	14.6	1.6	1
$\rho$	769	33.489	1.4	1
$\Delta$	1202			
$n\Delta\pi$		0.35	0.8	1
$n\Delta\rho$		20.45	1.35	2

The  $\pi$ - and  $\rho$ -transition strengths are given by

$$v_\pi(K) = -\frac{g_\pi(K)f_{n\Delta\pi}(K)}{2m_n m_\pi} \left[ \frac{1}{2\epsilon_\pi^2} + \frac{1}{2\epsilon_\pi(m'_\Delta - m_n + \epsilon_\pi)} \right] K^2, \quad (3a)$$

and

$$v_\rho(K) = -\frac{f_\rho(K)f_{n\Delta\rho}(K)}{2m_n m_\rho} \left[ \frac{1}{2\epsilon_\rho^2} + \frac{1}{2\epsilon_\rho(m'_\Delta - m_n + \epsilon_\rho)} \right] K^2. \quad (3b)$$

The masses of the nucleon, pion,  $\rho$ , and the  $\Delta$  in the nuclear medium are given by  $m_n$ ,  $m_\pi$ ,  $m_\rho$ , and  $m_\Delta$ . The energy-dependent coupling parameters are parametrized by the momentum convergent monopole or dipole form factors,

$$f_\alpha(K) = f_\alpha \left[ \frac{\Lambda_\alpha^2 - m_\alpha^2}{\Lambda_\alpha^2 + K^2} \right]^{n_\alpha}, \quad (4)$$

where  $\alpha = n, \pi, \rho, \Delta, n\Delta\pi, n\Delta\rho$ ,  $f_\pi \equiv g_\pi$ , and  $f_\rho = 6.1g_\rho$ . The values of these parameters obtained from R. Machleidt [12] are given in Table I. These interactions are similar to those used by Jain and Santra [13] except that Machleidt's interactions are generalized to include the nucleon-isobar mass difference. Equation (2a) is called the spin-longitudinal term because classically it becomes maximal when the momentum transfer is longitudinal to the spin and transition spin, whereas Eq. (2b) is called spin transverse because classically it maximizes for the spins transverse to the momentum transfer. Therefore,  $\pi$  exchange is associated with the spin-longitudinal term and  $\rho$  exchange is associated with the spin-transverse term. It will be seen in our calculations that the  $\pi$ -exchange effects are associated with the forward-backward directions in the pion angular distributions, whereas the  $\rho$ -exchange effects are more associated with the transverse directions in the same distributions. Plots of the  $\pi$ - and  $\rho$ -transition interaction strengths as given in Eqs. (3a) and (3b) as a function of momentum transfer are shown in Fig. 1.

As explained in Ref. [15], for producing  $\Delta$  isobars in the target nucleus, the interaction in configuration space in terms of the nucleus-nucleus separation distance  $\mathbf{r}$ , the target nucleon coordinate  $\xi_\Delta$ , and projectile nucleon coordinate  $\xi_p$  is obtained by taking the Fourier transform of the momentum-space interactions

$$v_{(\pi)}(\mathbf{r}, \xi_p, \xi_\Delta) = \frac{1}{(2\pi)^3} \int d^3K e^{i\mathbf{K} \cdot (\mathbf{r} - \xi_p - \xi_\Delta)} v_{(\pi)}(\mathbf{K}), \quad (5)$$

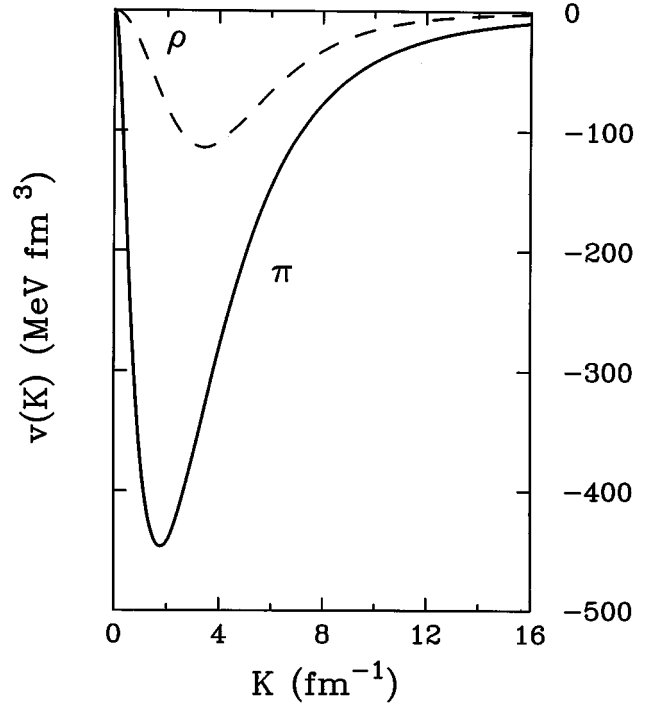


FIG. 1. Strengths of the  $\pi$ - and  $\rho$ -transition interactions  $v_\pi(K)$  (full line) and  $v_\rho(K)$  (dashed line) as functions of momentum transfer.

and then expanding the plane-wave, spin operator combinations into angular momentum multipoles containing rotational and tensor functions of the momentum  $\hbar\mathbf{K}$ , and formally integrating over the momentum solid angle giving [15]

$$v(\mathbf{r}, \xi_p, \xi_\Delta) = v_\pi(\mathbf{r}, \xi_p, \xi_\Delta) - v_\rho(\mathbf{r}, \xi_p, \xi_\Delta), \quad (6)$$

where the minus sign comes from an expansion of the transverse term (2b) into spherical operator components. The  $\pi$ - and  $\rho$ -exchange interactions in terms of the multipole expansion are given by

$$v_\pi(\mathbf{r}, \xi_p, \xi_\Delta) = \sqrt{4\pi}(2/\pi) \sum_{k_p k_\Delta L} i^{k_p - k_\Delta - L} \hat{k}_p \hat{k}_\Delta \begin{pmatrix} k_p & k_\Delta & L \\ 0 & 0 & 0 \end{pmatrix} \times \int K^2 dK v_\pi(K) [\mathbf{T}_{k_p}^s(K \xi_p)] \times \mathbf{T}_{k_\Delta}^s(K \xi_\Delta) \cdot \mathbf{T}_L(K \mathbf{r}), \quad (7a)$$

$$v_\rho(\mathbf{r}, \xi_p, \xi_\Delta) = \sqrt{4\pi}(2/\pi) \sum_{k_p k_\Delta L} i^{k_p - k_\Delta - L} \hat{k}_p \hat{k}_\Delta \times \sum_{\kappa=\pm 1} \begin{pmatrix} k_p & k_\Delta & L \\ \kappa & -\kappa & 0 \end{pmatrix} \int K^2 dK v_\rho(K) \times [\mathbf{T}_{k_p}^{s(+\kappa)}(K \xi_p) \times \mathbf{T}_{k_\Delta}^{s(-\kappa)}(K \xi_\Delta)] \cdot \mathbf{T}_L(K \mathbf{r}), \quad (7b)$$

where  $\mathbf{k}_p$  is the angular momentum transferred to the  $p$ th nucleon in the projectile,  $\mathbf{k}_\Delta$  is the angular momentum transferred to the  $t$ th nucleon in the target, and  $\mathbf{L} = \mathbf{k}_p + \mathbf{k}_\Delta$  is the total angular momentum transferred by the interaction. As

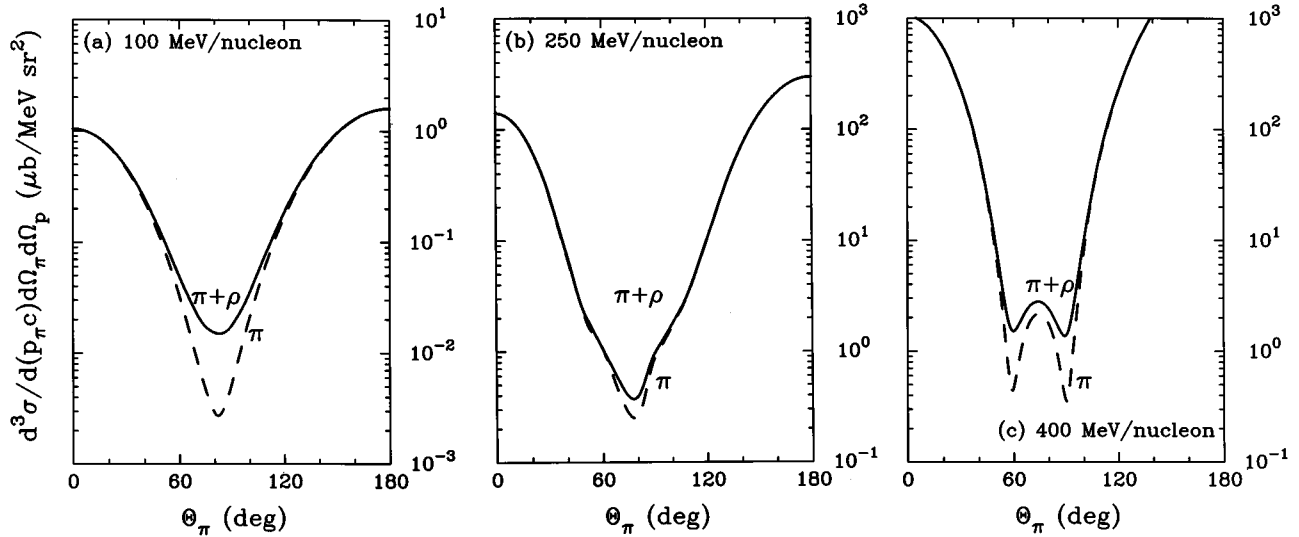


FIG. 2. (a) Triple differential cross sections in the exclusive reaction  $^{12}\text{C}+^{12}\text{C}\rightarrow^{12}\text{C}+^{12}\text{C} (15.11 \text{ MeV}) + \pi^0$  as a function of pion angle in the nucleus-nucleus c.m. frame at 100 MeV/nucleon incident laboratory energy. The full curve corresponds to coherent contributions coming from the  $(\pi + \rho)$ -transition interactions and the dashed curve corresponds to the  $\pi$ -transition interaction only. (b) Same as (a) except at 250 MeV/nucleon. (c) Same as (a) except at 400 MeV/nucleon. All curves are calculated under the conditions that  $t_\pi = 60 \text{ MeV}$ ,  $\phi_\pi = 0^\circ$ ,  $\Theta_\rho = \Phi_\rho = 0^\circ$ .

described in previous work [6,8,9], the expressions (7a) and (7b) are inserted into a second-order resonant amplitude between nuclear states to obtain the overall amplitude for  $\Delta$  formation and decay in either nucleus. Also in that work, the tensors in Eqs. (7a) and (7b) are described, but suffice it to say that they are various linear combinations of angular momentum coupled products of spherical Bessel functions, spherical harmonics, and spin operators in the spherical basis. The interactions (7a) and (7b) explicitly show that the Fourier transforms of the parallel and transverse interaction strengths (2a) and (2b) are distributed over various multipoles of momentum transfer in configuration space.

After insertion of Eqs. (7a) and (7b) into the nuclear matrix elements, the amplitudes are analytically solved and, for example, the target-generated pion amplitude

$$A_{T(\Delta)\rightarrow T\pi}^{p*} = \sum_{J_T M_T} A_{J_T J_P}^{M_T M_P}(\mathbf{K}_P) A_{J_T}^{M_T}(\mathbf{k}_\pi), \quad (8)$$

which is the product of the  $\Delta$ -formation amplitude  $A_{J_T J_P}^{M_T M_P}(\mathbf{K}_P)$  as a function of projectile-momentum transfer  $\hbar\mathbf{K}_P$  and the target decay amplitude  $A_{J_T}^{M_T}(\mathbf{k}_\pi)$  which generates a pion of momentum  $\hbar\mathbf{k}_\pi$ , and are summed over the intermediate angular momentum multipoles  $J_T$  and  $M_T$ . As described previously [6,8,9], it is in the formation amplitude where the  $\pi$ - and  $\rho$ -exchange terms give rise to parallel and transverse angular momentum coupled nuclear form factors. The parallel ( $\pi$ ) and transverse ( $\rho$ ) formation amplitudes are themselves a multipole expansion over the total nuclear angular momentum  $\mathbf{L} = \mathbf{J}_T + \mathbf{J}_P$  as

$$A_{J_T J_P}^{M_T M_P(\pi)}(\mathbf{K}) = v_\pi(K) A_{J_T J_P}^{t_z(\pi)} \sum_L H_{J_T J_P L}^\parallel(K) \Theta_{J_T J_P L}^{M_T M_P}(\hat{\mathbf{K}}), \quad (9a)$$

and

$$A_{J_T J_P}^{M_T M_P(\rho)}(\mathbf{K}) = v_\rho(K) A_{J_T J_P}^{t_z(\pi)} \sum_L H_{J_T J_P L}^\perp(K) \Theta_{J_T J_P L}^{M_T M_P}(\hat{\mathbf{K}}), \quad (9b)$$

where the parallel and transverse coupled form factors  $H_{J_T J_P L}^\parallel(K)$  and  $H_{J_T J_P L}^\perp(K)$  and the constant  $A_{J_T J_P}^{t_z(\pi)}$  are given in Ref. [6]. The angular function

$$\Theta_{J_T J_P L}^{M_T M_P}(\hat{\mathbf{K}}) = \begin{pmatrix} J_T & J_P & L \\ M_T & M_P & -(M_T + M_P) \end{pmatrix} Y_L^{-(M_T + M_P)}(\hat{\mathbf{K}}). \quad (10)$$

It should be mentioned that the terminology ‘‘nuclear form factor’’ as used in particle-hole calculations is a matrix element of an interaction expanded in multipoles taken between nuclear states and reduces to an interaction matrix element of single-particle, single-hole states. The nuclear form factors obtained in this work are essentially identical to the nuclear form factors discussed by Glendenning [14].

The main impact of the  $\rho$ -exchange transition interaction can be seen in Fig. 2, which are calculations of the exclusive pion angular distributions over the range of incident energies of 100, 250, and 400 MeV/nucleon for  $^{12}\text{C}+^{12}\text{C}\rightarrow^{12}\text{C}+^{12}\text{C}+\pi^0$  in the nucleus-nucleus c.m. The curve marked  $\pi + \rho$  is the full calculation with both  $\pi$ - and  $\rho$ -transition interactions included, whereas the curve marked  $\pi$  contains the  $\pi$ -transition interaction alone. As seen in Fig. 2, mild enhancements occur in the transverse pion directions approximately around  $\theta_\pi = 80^\circ$ . This region is very interesting because it is also the region where the projectile-generated pion amplitude interferes coherently with the target-generated pion amplitude [10].

The points at  $\theta_\pi = 0^\circ$  and  $180^\circ$  are also special because the  $\rho$  component of the three-body amplitude is identically zero. To show this, consider the overall amplitude of Eq. (8). Since the decay amplitude is proportional to the spherical

harmonic  $Y_{J_T}^{M_T}(\hat{\mathbf{k}}_\pi)$ , then for forward and backward angles  $A_{J_T}^{M_T} \propto \delta_{M_T,0}$ , so the only nonzero contribution to the overall amplitude is when  $M_T=0$ . In the present calculation, the intermediate, giant spin-isospin, excited state multipoles of target and projectile have been chosen to be the physical states  $L_T=0$ ,  $L_P=0$ , and therefore  $J_T=J_P=1$ . This choice then limits the total angular momentum values to  $L=0,1,2$ . Therefore, the sums over  $L$  in Eqs. (9a) and (9b) are limited to these values only.

Since the pion distributions are restricted to projectile forward angles,  $\Theta_P=0^\circ$  which means that the projectile momentum transfer is also in the forward direction, then for  $\Theta_K=0^\circ$ , the spherical harmonic in Eq. (10) reduces to

$$Y_L^{-(M_T+M_P)}(\hat{\mathbf{K}}) = \frac{\hat{L}}{\sqrt{4\pi}} \delta_{(M_T+M_P),0}.$$

With the additional restriction that  $M_T=0$  which comes from the decay amplitude, then  $M_T=M_P=0$  is the only possible nonzero contribution provided by the transverse formation amplitude. The transverse coupled form factor

$$H_{J_T J_P L}^\perp(K) = \sum_{\kappa=\pm 1} G_{J_T L_T}^{\perp(\kappa)}(K) \hat{J}_T \hat{J}_P \hat{L} \begin{pmatrix} J_T J_P L \\ \kappa - \kappa 0 \end{pmatrix} G_{J_P L_P}^{\perp(-\kappa)}. \quad (11)$$

For  $J_T=J_P=1$  and  $L_T=L_P=0$ , the uncoupled transverse form factors become

$$G_{J_T L_T}^{\perp(\kappa)}(K) = G_{J_P L_P}^{\perp(-\kappa)}(K) = \sqrt{\frac{1}{3}} F_{L_T=0}(K), \quad (12)$$

where  $F_{L_T=0}(K)$  is the nuclear form factor generated by the particle-hole model and given by Eq. (18) in Ref. [6]. What is now important is that the uncoupled transverse form factors are independent of the sum over  $\kappa$ . Therefore, when the sum over  $L$  is taken in Eq. (5), and picking up a factor of  $\hat{L}$  and a 3- $j$  symbols from each of Eqs. (6) and (7), the orthogonality of the 3- $j$  symbols gives

$$\sum_{L=0}^2 \hat{L}^2 \begin{pmatrix} J_T J_P L \\ M_T M_P 0 \end{pmatrix} \begin{pmatrix} J_T J_P L \\ \kappa - \kappa 0 \end{pmatrix} = \delta_{M_T, \kappa} \delta_{M_P, -\kappa}. \quad (13)$$

Since the  $\kappa$  values are restricted to  $\kappa=\pm 1$ , and since  $M_T=M_P=0$ , then by orthogonality in Eq. (13), the  $\rho$  component of the target-generated  $\Delta$  amplitude  $A_{J_T J_P}^{M_T M_P(\rho)}(\mathbf{K}_P)=0$  for projectiles scattered in the forward direction ( $\Theta_P=0^\circ$ ) under the restriction that  $\theta_\pi=0^\circ$  or  $180^\circ$ . A similar argument also holds for the projectile-generated  $\Delta$  amplitude  $A_{J_P J_T}^{M_P M_T(\rho)}(-\mathbf{K}_T)$  for targets scattering in the backward angle ( $\Theta_T=180^\circ$ ). Here  $\hbar\mathbf{K}_P$  and  $\hbar\mathbf{K}_T$  are, respectively, the projectile- and target-momenta transfer (see Ref. [11]). Therefore, the  $\rho$  component of the three-body amplitude is zero for the extreme angles of forward and backward pions and forward projectile and backward target angles. The vanishing of the pion production cross section at  $\theta_\pi=0^\circ$  for transverse interactions is reminiscent of a similar result obtained Ref. [3] for charge-exchange reactions. This result explains why  $\rho$  contributions are likely to be seen only in the

midregion around  $\theta_\pi=80^\circ$ . (As discussed previously in Ref. [10], the asymmetric shift from  $\theta_\pi=90^\circ$  is due to the three-body nature of the kinematics and phase-space and the energy dependencies in the  $\Delta$  width.) This also means that only the  $\pi$ -exchange interaction contributes to the forward-backward angles in the pion-angular distributions. Furthermore, since the pion-energy distributions are calculated under the restrictions of forward-scattered projectile and forward-angle pions, then the pion-energy distributions for all pion energies have no  $\rho$ -exchange contribution either. Pion-energy distribution calculations have confirmed this. Therefore, the pion-energy distributions under forward-angle restrictions are a clean picture of  $\pi$ -exchange contributions only within the Born approximation. Finally, we can see qualitatively that the  $\rho$ -exchange contribution is relatively mild because a glance at Fig. 1 shows that the strength of the  $\rho$ -exchange interaction is much smaller than the  $\pi$ -exchange interaction except for extremely small or large values of momentum transfer. At the incident energies considered here, the projectile momentum transfers are in a range from approximately  $0.9$  to  $2.8 \text{ fm}^{-1}$ , where the  $\rho$ -exchange strengths are decidedly smaller than the  $\pi$ -exchange strengths. The  $\rho$ -exchange effect provides only a mild enhancement to the  $\pi$ -exchange contribution in the midangular region of the pion-angular distributions.

There is no dominant channel that explains the mild enhancement seen in Fig. 2, however, the following is a simplifying explanation. First, the cross section, as described in Eq. (28) in Ref. [6] for pion production is proportional to

$$\sum_{\substack{J_P J_T \\ M_P M_T}} \left| \frac{A_{T(\Delta) \rightarrow T\pi}^{J_P M_P} + A_{P(\Delta) \rightarrow P\pi}^{J_T M_T}}{\epsilon_\pi + m_n c^2 - m_\Delta' c^2 + i\Gamma_\Delta'(\epsilon_\pi)/2} \right|^2, \quad (14)$$

where the sums are over final states. The calculation in Fig. 2 was done under the restriction that  $J_P=J_T=1$  so that  $M_T=0 \pm 1$  and  $M_P=0 \pm 1$  which means that there are  $3 \times 3 = 9$  multipole amplitudes running over all possible values of  $M_T$  and  $M_P$ . If we consider the 100 MeV/nucleon angular distribution where  $t_\pi=60 \text{ MeV}$  and choosing the angle  $\theta_\pi=80^\circ$ , we have compared the nine amplitudes with and without the  $\rho$ -exchange effect. For reasons of simplicity, set the projectile-production amplitude  $A_{P(\Delta) \rightarrow P\pi}^{J_T M_T}=0$ , so that we can compare the target-production amplitude  $A_{T(\Delta) \rightarrow T\pi}^{J_P M_P}$  with and without the  $\rho$ -exchange effect. The numerator in Eq. (14) then reduces to

$$3 \sum_{M_P=-1}^1 |A_{T(\Delta) \rightarrow T\pi}^{M_P(\pi)} - A_{T(\Delta) \rightarrow T\pi}^{M_P(\rho)}|^2, \quad (15)$$

where 3 is the factor coming from the sum over  $M_T$  and the amplitudes labeled ( $\pi$ ) and ( $\rho$ ) are due to the  $\pi$ - and  $\rho$ -exchange terms and the minus sign comes from the sign in Eq. (6). Expression (15) is a sum over positive terms because the net amplitude is squared. It turns out that the  $\pi$  amplitude contributes only for  $M_P=0$  and the  $\rho$  amplitude only for  $M_P=\pm 1$ . In detail,  $A_{T(\Delta) \rightarrow T\pi}^{M_P(\pi)}=0$  at  $M_P=\pm 1$  for two reasons. Since the projectile is measured at forward angles, either the spherical harmonic in Eq. (10) is zero when  $M_T+M_P \neq 0$  or for the special case that  $M_T=\pm 1$  and  $M_P=$

$\mp 1$  when the spherical harmonic is not zero, the sum over  $L$  in Eq. (9a) is zero due to cancellations caused by orthogonality relations in  $H_{J_T J_P L}^{\parallel}(K)$ . Therefore, the only contribution from a longitudinal or  $\pi$  amplitude for forward going projectiles occurs only when  $M_P=0$ . On the other hand, the  $\rho$  amplitude  $A_{T(\Delta) \rightarrow T\pi}^{M_P(\rho)}=0$  for  $M_P=0$ , again due either to the spherical harmonic being zero at forward angles or to the orthogonality conditions in  $H_{J_T J_P L}^{\parallel}(K)$ . Perversely, the only contributions from a transverse or  $\rho$  amplitude for forward going projectiles occurs only when  $M_P=\pm 1$ . Therefore, there is only one nonzero term in Eq. (15) for  $M_P=\pm 1$  coming only from the  $\rho$  contribution and only one nonzero term in Eq. (15) coming from the  $M_P=0$   $\pi$  contributions. When these amplitude values are squared and then added, a small enhancement due to the  $\rho$ -contribution results.

The amplitude for projectile  $\Delta$  production is not as simple as the target amplitude because the target, which is scattered, comes out near the backwards direction in the nucleus-nucleus, center-of-momentum frame, but not at  $\Theta_T=180^\circ$ . However, we painstakingly examined the nine multipoles and all the contributing factors and found that a large majority of these multipoles add in phase when the  $\rho$  contribution is included. These changes in sign come about from a number of sources. First, the angular function  $\Theta_{J_T J_P L}^{M_T M_P}(\hat{\mathbf{K}})$  is a product of a 3- $j$  symbol and a spherical harmonic Eq. (10), which individually can introduce minus signs depending on the  $M$ -values. Next, the parallel and transverse form factors  $H_{J_T J_P L}^{\parallel}(K)$  and  $H_{J_T J_P L}^{\perp}(K)$  contain different 3- $j$  symbols that can contribute different signs. Finally, there are parity phase factors  $(-)^{L_A+1}$  and  $(-)^{L_A}$  that can provide negative signs. When the nine multipoles for the total amplitude in Eq. (14) are considered, again, the  $\pi$  contributes only to the  $M_P=0$  multipole, whereas the  $\rho$  exchange contributes only to the  $M_P=\pm 1$  multipoles of the target-generated  $\Delta$ 's. Thus, the projectile-generated amplitudes are modified in which a large majority of the multipoles increase with inclusion of the  $\rho$  contribution. It turns out, however, that when the target- and projectile-generated amplitudes are added, six of the nine multipoles for  $M_P=\pm 1$  and  $M_T=0\pm 1$  exactly or approximately cancel because they are exactly or approximately out of phase. The three remaining multipoles for  $M_P=0$  and  $M_T=0\pm 1$  are the only multipoles of significance and an examination of these values shows that two of the multipoles that add in phase are larger than the remaining out of phase multipole. The final result is that there is a net in-phase increase when the  $\rho$  contribution is included and hence the cross section is slightly enhanced in the  $\rho$ -sensitive region around  $\theta_\pi=80^\circ$ . This occurs for all the angular distributions shown in Fig. 2.

An interesting question arises about the role of the  $\rho$ -exchange contribution between nuclei as compared to its contribution in the bare  $nn \rightarrow n\Delta$  channel. This effect has been studied in Ref. [16] within the Bonn model. In that work, a modified version of the Bonn model in momentum space, referred to as ‘‘peripheral,’’ is used for comparison. This version provides less short-range repulsion by suppressing the  $\rho$  exchange in the  $n\Delta$  channel (as well as applying a weaker  $\omega$  coupling). As a consequence, the  $nn \rightarrow n\Delta$  differential cross section is enhanced without the  $\rho$ -exchange con-

tribution; whereas, with the  $\rho$ -exchange contributions, the cross section is diminished. The diminution is due to the fact that when the  $\pi$  and  $\rho$  interactions are reexpressed as spin-spin and tensor terms [12], the tensor term in the  $\rho$  interaction is opposite that of the tensor term in the  $\pi$  interaction. The spin-spin terms though, add up coherently, but since the tensor terms are stronger than the spin-spin terms, there is a net diminution of the interaction. How is this result reconciled with the slight enhancement seen in our calculation? As it happens with any multipole expansion, we have restricted these sums to certain channels of physical interest. Since both the  $\pi$  and  $\rho$  strengths have been distributed among their own multipoles, and because of the restrictions placed on the multipole values, then neither strength is fully developed and it is plausible that we might find a  $\rho$  enhancement for a restricted set of multipole values.

To elucidate, the angular momentum couplings in this work lead to a stacked set of values moving from the microscopic, particle-hole couplings through to the macroscopic coupling for each nucleus and finally to the internuclear coupling to produce a total angular momentum. The couplings are the stacked set

$$\mathbf{L}_A = \mathbf{l}_p + \mathbf{l}_h, \quad (16a)$$

$$\mathbf{S}_A = \mathbf{s}_p + \mathbf{s}_h, \quad (16b)$$

$$\mathbf{J}_A = \mathbf{L}_A + \mathbf{S}_A, \quad (16c)$$

$$\mathbf{L} = \mathbf{J}_A + \mathbf{J}_{A'}. \quad (16d)$$

For the  $\Delta$  nucleus,  $s_\Delta = \frac{3}{2}$  and  $s_h = \frac{1}{2}$ , so  $S_A = 1, 2$ . Only the physical spin  $S_A = 1$  was considered in the present calculation. As in any shell-model calculation, the microscopic particle-hole states are usually truncated and this then truncates the possible macroscopic nuclear angular momenta values given by Eqs. (16a)–(16d). Furthermore, out of the truncated set of values, we chose only certain values due to physical interest. In the present calculation, we included only the two valence excited states ( $1p_\Delta, 1p^{-1}$ ) and ( $2p_\Delta, 1p^{-1}$ ) and the two core excited states ( $1s_\Delta, 1s^{-1}$ ) and ( $2s_\Delta, 1s^{-1}$ ). Since only intermediate-excited-state giant monopole modes were considered, we set  $L_A = 0$ . Because a 3- $j$  symbol  $\begin{pmatrix} l_\Delta & l_A & l_h \\ 0 & 0 & 0 \end{pmatrix}$  appears in the microscopic  $\Delta$ -formation factor, setting  $L_A = 0$  requires that  $l_\Delta = l_h$  and thus determines the microscopic set of particle-hole states as chosen above.

Because excited spin modes were the only modes considered ( $L_T = L_P = 0$ ), then the nuclear angular momenta were restricted to  $J_T = J_P = 1$ . This further restricted the total angular momenta to  $L = 0, 1, 2$ . [In the actual calculation only even-values of  $L$  survive because of orthogonality and symmetry properties of 3- $j$  symbols associated with the coupled form factors  $H_{J_T J_P L}^{\parallel}(K)$  and  $H_{J_T J_P L}^{\perp}(K)$ .] Therefore, the truncation of the microscopic particle-hole states and the interest in the physical giant resonant spin modes leads to a highly restricted calculation which limits the full strength of both the  $\pi$ - and  $\rho$ -exchange interactions.

And finally, the energy-dependent free  $\Delta$  width  $\Gamma'_\Delta(\epsilon_\pi)$  in the Breit-Wigner denominator (BWD) in Eq. (14) follows the parametrization of Guet, Soyeur, Bowlin, and Brown [17] and has been discussed in Ref. [11]. As discussed, the

free width was modified to  $\Delta$ -in-nuclei values which were taken from Ref. [18], where the  $\Delta$  at resonance has a mass 30 MeV lower and a width 40 MeV larger inside nuclei. This parametrization rests on a low-energy approximation, but was used to begin these calculations so that at least an estimate of the magnitude and shape of pion distributions can be made. Since the present calculation assumes the Born approximation, medium effects on the  $\Delta$  resonance are not yet fully included. However, the calculations at present are valuable in assessing the relative effects due to the  $\pi$  and  $\rho$  contributions. A fuller treatment of the complete energy dependence will be the subject of future work. As a test separate calculations of these widths for all the pion angular distributions in Fig. 2 were done and show that they are almost flat over the pion angles and never exceed the value of approximately 170 MeV in the case of 400 MeV/nucleon. Furthermore, calculations of  $[1/\text{BWD}]^2$  over the same angles, show that the effect of the resonance denominator is even flatter. This means that the energy dependence is almost constant as far as the pion angular distributions are concerned. When a comparison of the  $\pi$  and  $\rho$  contributions for pion angular distributions is made for fixed pion energy  $t_\pi$  and angle  $\theta_\pi$ , the energy dependence is essentially canceled out so a relative comparison is meaningful.

### III. CONCLUSIONS

The  $\rho$ -exchange transition interaction which is essentially the spin-transverse component of the total interaction only

marginally enhances the pion angular distributions in the midregions of the angular distributions calculated for excitations to giant spin modes under the Born approximation. Because of angular momentum symmetry properties, the  $\rho$ -exchange interaction gives no contribution to the pion energy distributions which are calculated under the restriction of forward-going projectile, backward-going target, and forward-angle pions in the nucleus-nucleus c.m. system. This means that under the Born approximation, pion energy distributions are a clean picture of  $\pi$ -exchange effects only. On the other hand, the pion angular distributions have no  $\rho$  contributions at extreme pion angles ( $\theta_\pi=0^\circ$  or  $180^\circ$ ). The  $\rho$  contributions are mainly seen in the midangular region. The angular momentum coupling involved in this calculation leads to a stacked set of angular momentum values and by truncating the microscopic particle-hole states as well as considering only certain excited giant resonant spin modes of interest, the calculation includes only those channels necessary to excite these states. The pion angular distributions then include only partial strengths of the  $\pi$ - and  $\rho$ -exchange interactions due to the truncation and selection of certain multipole values. To within the excited multipoles selected, it is seen that collectivity is strong in the longitudinal channel and quite weak in the transverse channel.

### ACKNOWLEDGMENTS

This author thanks J. Papillon for his help with computer support.

- 
- [1] P. Fernández de Córdoba, E. Oset, and M. J. Vicente-Vacas, Nucl. Phys. **A592**, 472 (1995).
  - [2] T. Udagawa, P. Oltmanns, F. Osterfeld, and S. W. Hong, Phys. Rev. C **49**, 3162 (1994).
  - [3] F. Osterfeld, B. Kämpfer, P. Oltmanns, and T. Udagawa, Nucl. Phys. **A577**, 237c (1994).
  - [4] V. Dmitriev, Nucl. Phys. **A577**, 249c (1994).
  - [5] E. Oset, P. Fernández de Córdoba, B. López Alvaredo, and M. J. Vicente Vacas, Nucl. Phys. **A577**, 255c (1994).
  - [6] P. A. Deutchman, Phys. Rev. C **45**, 357 (1992).
  - [7] Khin Maung Maung, P. A. Deutchman, and R. L. Buvel, Can. J. Phys. **70**, 202 (1992).
  - [8] P. A. Deutchman, Phys. Rev. C **47**, 881 (1993).
  - [9] P. A. Deutchman and G. Q. Li, Phys. Rev. C **47**, 2794 (1993).
  - [10] P. A. Deutchman and B. Erasmus, Phys. Rev. C **51**, R5 (1995).
  - [11] P. A. Deutchman, Can. J. Phys. **74**, 634 (1996).
  - [12] R. Machleidt, Adv. Nucl. Phys. **19**, 189 (1989); **19**, 354 (1989); **19**, 214 (1989).
  - [13] B. K. Jain and A. B. Santra, Nucl. Phys. **A500**, 681 (1989).
  - [14] N. Glendenning, *Direct Nuclear Reactions* (Academic, New York, 1983), p. 146.
  - [15] F. Pétrovich, Nucl. Phys. **A251**, 143 (1975); F. Petrovich, R. J. Philpott, A. W. Carpenter, and J. A. Carr, *ibid.* **A425**, 609 (1984).
  - [16] F. Sammarruca, Phys. Rev. C **50**, 652 (1994).
  - [17] C. Guet, M. Soyeur, J. Bowlin, and G. E. Brown, Nucl. Phys. **A494**, 558 (1989); C. Guet (private communication).
  - [18] M. Roy-Stephan, Nucl. Phys. **A482**, 373c (1988); E. J. Moniz, *ibid.* **A374**, 557c (1982).